

X-625-72-219

PREPRINT

NASA TM X- 66013

TRANSITION REGION RESPONSE OF THE SYMMETRIC DOUBLE PROBE AND ITS APPLICATION IN THE LOWER IONOSPHERE

EDWARD P. SZUSZCZEWICZ

JULY 1972

(NASA-TM-X-66013) TRANSITION REGION
RESPONSE OF THE SYMMETRIC DOUBLE PROBE AND
ITS APPLICATION IN THE LOWER IONOSPHERE
E.P. Szuszczewicz (NASA) Jul. 1972 23 p

N72-32400

Unclas

CSCL 04A G3/13 41995

GSFC

GODDARD SPACE FLIGHT CENTER
GREENBELT, MARYLAND



TRANSITION REGION RESPONSE OF THE SYMMETRIC DOUBLE PROBE
AND ITS APPLICATION IN THE LOWER IONOSPHERE

Edward P. Szuszczewicz

Laboratory for Planetary Atmospheres

National Aeronautics and Space Administration

Goddard Space Flight Center

Greenbelt, Maryland 20771

ABSTRACT

The technique of the symmetric double-probe readily lends itself to the "in situ" measurement of plasma temperature in the ionospheric D-region because it can lead to meaningful results under relatively high collision frequencies where the Langmuir probe has been observed to fail. For a completely thermalized plasma and over parametric ranges $0.1 \leq \lambda_{ia}/R_p \leq 100$ and $0.004 \leq R_p/\lambda_D \leq 100$, where λ_{ia} is the ion-atom mean free path, R_p is the probe radius and λ_D is the Debye length, it is shown that the modification to the original collision-free double-probe theory of Johnson and Malter for the determination of electron temperature is never greater than $\pm 12\%$, with a value of $(8 \pm 2)\%$ nominally

applicable in the case of D-region diagnostics. This technique has been successfully operated on a Nike-Cajun payload flown at mid-day from White Sands, New Mexico to an apogee of 78.5 km. The associated electronics and deployed double-probe configuration are presented, and a current-voltage characteristic collected in the ascent stage at 73.7 km is briefly discussed. The values of electron temperature indicated by the sampled data are approximately 30% higher than those predicted by theory for the anticipated state of thermal equilibrium with the ambient neutrals. The importance, however, is that these values, of the order of 300°K, are the lowest ever reported by any "in situ" method operative in D-region and consequently point out the strong potential of the double-probe technique in future applications to regions of planetary ionospheres which cannot be considered as collision-free.

I. INTRODUCTION

Electrostatic probes are widely used as diagnostic tools for determining the local properties of laboratory, ionospheric and interplanetary plasmas. When a variable voltage is applied between a probe and its reference electrode, the resulting current-voltage characteristic can, under appropriate circumstances, yield a measure of the plasma density and its temperature. The correct measure of these plasma parameters can occur only when the probe response in a particular plasma environment is well understood. For some time only the continuum and collision-free regimes were theoretically and experimentally well in hand but recent developments have contributed significantly to the understanding of probe behavior in the transition region, that is, the region between the collision-free and continuum limits.

The developments in the understanding of transition region probe response are particularly important to the application of probe diagnostics in the ionospheric D-region where the ion-atom and electron-atom mean free paths can be comparable to probe and/or rocket dimensions. It is this particular application which will be emphasized here in connection with the well known diagnostic technique of the floating symmetric double probe. Although attention is directed to D-region applications, the theoretical foundations of the technique apply whenever the probe and plasma parameters are such that the conditions of the transition regime are obtained. These conditions are generally encountered whenever

the ambient gas pressure exceeds an approximate limiting value of 10μ Hg. In the cases of Martian and Venutian ionospheres these conditions are met at altitudes nominally less than 110 km.

In the succeeding sections the influences of ion-atom collisions on the current-voltage characteristic of a symmetric double-probe system will be established in connection with the determination of the temperature of a completely thermalized plasma. The manner in which this technique can be implemented for a rocket-borne experiment will be described and an experimental current-voltage characteristic obtained in the Earth's lower ionosphere will be presented and briefly discussed.

II. THEORETICAL CONSIDERATIONS

In most applications of probe diagnostics there is an electrode in good electrical contact with the plasma which can be utilized as a reference point for introducing a bias voltage on a probe. In laboratory plasmas this electrode can be the anode or cathode of a discharge or the metallic container or limiter of a given plasma volume. In these instances, when a good fixed-potential reference point is available, the technique of the single probe,¹ the Langmuir probe, can generally be utilized in a straightforward fashion. However, there are instances in which such a reference point is not available; typical examples are inductively-coupled hf discharges with nonconducting boundaries and ionospheric plasmas. In such cases it becomes necessary to utilize the floating double-probe technique

of Johnson and Malter², who originally applied the method to the study of decaying plasmas.

It should be noted that the use of the Langmuir probe technique in ionospheric applications is a special case of the double-probe method. This special case is a limiting one in which the ratio of the probe areas must for all practical purposes be considered infinite in order for the analysis scheme of the simple Langmuir probe to be applicable³. In this instance the larger probe is the rocket or satellite itself.

The general configuration and a corresponding dimensionless current-voltage characteristic of the floating double-probe technique is illustrated in Fig. 1. The illustration is specifically that of a symmetric double-probe system with the probes being of cylindrical geometry and operating in a completely thermalized homogeneous plasma under conditions of orbital-motion-limited currents.^{4,5} The method employs two identical probes separated by a variable bias voltage and an electrometer, and the two-electrode system is floated, i. e. the probes and associated circuitry are electrically isolated from any other electrodes which may be in contact with the plasma. In the case of ionospheric investigations the other electrode is the vehicle or the payload. When the current I is plotted as a function of the applied voltage V the resulting characteristic is point symmetric about the origin as illustrated in this figure.

The procedure for determining the electron temperature T_e from the parameters of the I-V curve under conditions of non-negligible ion-atom collision frequencies is discussed in the work of Kirchhoff, Peterson and Talbot⁶. This procedure is summarized by

$$T_e = \frac{e}{k} \frac{i_1 \cdot i_2}{(i_1 + i_2)} \frac{(1 + \sigma)}{(dI/dV)_{V=0}} \quad (1)$$

where it can be seen that the temperature is dependent upon the extrapolated values of the saturation currents⁷, i_1 and i_2 (see Fig. 1), as well as on the slope of the curve at the origin. (The work of Burrows⁸ indicates that in cases of asymmetric I-V characteristics the slope should be evaluated at the inflection point of the curve.) The parameter σ is a function of the plasma density and temperature and of the probes' size and geometry — it is this parameter which takes into account collision effects in the transition region.

Figure 2 presents a plot of the temperature correction parameter σ as a function of R_p/λ_D where R_p is the probe radius and λ_D is the electron Debye length. The calculations which yielded the results in this figure were based on the transition region analysis of Kirchhoff, et al.,⁶ and apply specifically to the case of cylindrical probes of length $L = 200 R_p$ immersed in a completely thermalized plasma with the dominant positive ion being of mass 30 amu. (As indicated by the work of Peterson and Talbot⁹, these results are relatively insensitive to the value of ion mass.) The running parameter is the ion-atom Knudsen number, λ_{ia}/R_p , where λ_{ia} is the ion-atom mean free path.

In addition to collision effects the parameter σ also modifies the results of the original theoretical model of Johnson and Malter² by accounting for the non-zero slope of the saturation portion of the current-voltage characteristic ($|eV/kT_e| \geq 5$ in Fig. 1). This is evident by considering the curve in Fig. 2 which corresponds to $\lambda_{ia}/R_p = 100$. This value of λ_{ia}/R_p has been shown by Kirchhoff, et al. to mark the lowest ion-atom Knudsen number for which the probe response can be properly described as collision-free. There are two types of behavior evident in this curve. σ maintains a constant value in the domain of orbital-motion-limited currents ($R_p/\lambda_D \leq 2.37$), while in the region $R_p/\lambda_D > 2.37$ σ is a monotonically decreasing function. The latter behavior is to be expected since increasing values of R_p/λ_D represent relative decreases in sheath size with a saturation current response that is correspondingly more flat. In the limit $R_p/\lambda_D \rightarrow \infty$ the slope of the saturation current would approach zero as would the value of σ . In this limit the form of Eq. (1) is identical to that which was obtained with the zero slope assumption in the original theory of Johnson and Malter.

As λ_{ia}/R_p decreases from 100, ion-atom collisions begin to play an increasing role with the general effect being a reduction in the current collected by the probe and a flattening of the current-voltage response in the saturation portion of the characteristic. The end result of the latter effect is a reduction in the value of σ as can be seen in all cases of Fig. 2 with an exception being the curve corresponding to $\lambda_{ia}/R_p = 0.1$ in the region $R_p/\lambda_D < 0.03$. In the exception the

collisions have eliminated any semblance of orbital-motion-limited behavior with the probe response being more like that of a sphere (i.e., increasing sheath size always results in increased current levels and a steeper current-voltage response in saturation regions of probe current) than a cylinder.

For D-region applications it is generally only necessary to consider the domain in Fig. 2 bounded by $0.1 \leq \lambda_{ia}/R_p \leq 1.0$ and $0.006 \lesssim R_p/\lambda_D \lesssim 0.022$ where these limits were obtained by taking the probe radius as 0.5 mm and by estimating λ_{ia} on the basis of the ion's mobility in the polarization limit.^{10, 11} The shaded region in Fig. 2 is therefore the one applicable to D-region analysis. A very convenient feature to be noted is that over the entire D-region the value of σ may be taken as 0.08 ± 0.02 thus eliminating any need for an accurate determination of the ion-atom mean free path at all points throughout the flight.

III. EXPERIMENT

Figure 3 illustrates the electronics system employed in the laboratory and ionospheric application of the floating double-probe technique described above. The electrometer had a dual-polarity semilogarithmic response over the current range 10^{-13} to 10^{-10} amperes with a rise time nominally equal to 20 ms. The sweep voltage impressed between the two probes had a total excursion of 1.0 V from -0.5 V to +0.5 V on a time scale of 3 sec. Direct current isolation of the probe circuitry was achieved by a voltage-to-frequency conversion of the electrometer and sweep generator outputs with these parameters being coupled to

the telemetry system through an isolation transformer. The use of the isolation transformer and teflon for all insulation and mountings achieved a dc isolation greater than 10^{12} ohms. This isolation decoupled the probes and their associated circuitry from the payload thus minimizing the possibility of perturbations resulting from changing skin potentials.

Figure 4 shows a scaled presentation of the deployed symmetric double-probe configuration which was flown on a Nike-Cajun (NASA 10.378) payload from White Sands, New Mexico in October 1971. The deployed configuration of the probes is such that their axes are colinear and perpendicular to the axis of the cylindrical payload. The probes were constructed from 1 mm diameter molybdenum rod and were 200 mm in length resulting in a length-to-diameter ratio equal to 200. The probe supports were lengths of stainless steel tubing machined to 5 mm O.D. These supports, which were maintained at the payload's skin potential were connected to the probes by means of coiled springs that functioned as shock absorbers at the time of deployment. In this arrangement there was an 18 cm separation between the nearest end of the probe and the payload circumference. Other on-board experiments were a Gerdien condenser for total ion density, a positive-ion mass spectrometer, and Faraday rotation for electron density (not illustrated). In the launch phase the probes and their supports were folded up at the illustrated pivot points to fit inside the nosecone. To accommodate the Faraday experiment the payload was spun up to a nominal rate

of 6 rps and the centrifugal force of the spinning payload provided the mechanism for probe deployment after nosecone release.

Figure 5 presents a sample of the telemetered data collected on the rocket payload which had an apogee of 78.5 km. The launch occurred at 1300 hours LT and these data were obtained during ascent at 73.7 km. The figure shows the outputs of the electrometer and sweep generator as well as that of a solar aspect sensor which was mounted on the lateral surface of the payload. The periodic modulation of the electrometer output is coupled directly to the spin frequency of the payload as evidenced by a comparison of the electrometer response with that of the solar aspect sensor. The portions of the curve most representative of the symmetric double-probe response to the ambient plasma, as a result of being least subject to the possible secondary influences of wake and photoemission asymmetries, are those corresponding to times at which the axes of the probes were simultaneously perpendicular to the payload-to-sun line and to the payload's velocity vector. These two events of perpendicularity were not coincident but were never separated by more than 20° in any given 360° payload rotation. In Fig. 5 the 20° intervals which overlap the two events of perpendicularity occur approximately within the time period marked by the responses (and midway between adjacent responses) of the solar aspect sensor. The linear I-V characteristic associated with the leading edges of these intervals between points A and B in Fig. 5 is presented in Fig. 6 where the analysis procedure described

earlier yields an electron temperature of approximately 320°K . This value is the lowest ever reported by any "in situ" technique operative in the ionospheric D-region and as such comes closest to being in agreement with the anticipated state of thermal equilibrium between electrons and the ambient neutral species. In the latter case the anticipated temperature at 74 km is approximately 220°K ¹².

The results shown in Fig. 5 and the corresponding determination of electron temperature are generally representative of all data collected on this flight with the qualification that the determined values of electron temperature were observed to vary with altitude and the periodic modulation in the ascent and descent phases showed different structures. These details will be presented and discussed elsewhere.

IV. COMMENTS AND CONCLUSIONS

It has been demonstrated that the effects of ion-atom collisions on the determination of electron temperature in a completely thermalized plasma can result in values of electron temperature which are lower than the actual value by as much as 12% if one employs the analysis scheme originally proposed by Johnson and Malter². Using the analysis procedure of Kirchhoff, et al.⁶ these effects have been properly taken into account with particular attention given to applications in the ionospheric D-region. In this connection it has been shown that without the need for an exact determination of ion-atom mean free path at every point of a payload trajectory the collision modification to the work of

C

Johnson and Malter is $8 \pm 2\%$. This result applies specifically to cylindrical probes of radius 0.5 mm but can be used for probe dimensions of reasonable variations without significant inaccuracies.

An initial flight of a symmetric double-probe system into the ionospheric D-region has shown satisfactory performance of the associated electronics and has yielded electron temperatures of the order 300°K . These values are the lowest ever reported by any "in situ" method operative in the lower ionosphere and indicate the strong potential of the double-probe technique in future studies of those ionospheric plasmas which cannot be considered as collision free.

ACKNOWLEDGEMENTS

As in any experiment which has moved through the stages of design, testing and flight there are a large number of people who have made contributions in one way or another. The author would especially like to thank Mr. D. Silbert whose electronics design expertise played a contributing role of major proportions. Sincere gratitude is also extended to Mr. G. Spaid for the many periods of helpful discussion which he provided throughout the entire program and to Mr. S. Evan for his careful construction of the electronics package. With sincere appreciation the author also wishes to acknowledge the opportunity and motivation provided by Dr. R. Goldberg and the support of Dr. A. Aikin. This program was carried out while the author was a Research Associate of the National Academy of Sciences/National Research Council.

REFERENCES

1. F. F. Chen, in Plasma Diagnostic Techniques, R. H. Huddleston and S. L. Leonard, Eds. (Academic Press, New York, 1965), p. 113.
2. E. O. Johnson and L. Malter, Phys. Rev. 80, 58 (1950).
3. E. P. Szuszcwicz, J. Appl. Phys. 43, 874 (1972).
4. J. G. Laframboise, University of Toronto Institute of Aerospace Studies Report No. 100 (1966) (unpublished).
5. Orbital-motion-limited current is that current collected by a probe when there are no barriers of effective potential which prevent incoming charged particles from reaching the probe.
6. R. H. Kirchhoff, E. W. Peterson and L. Talbot, AIAA J. 9, 1686 (1971).
7. As a matter of convenience the values of i_1 and i_2 at $V=0$ have been taken at the intersections of the corresponding linearly extrapolated saturation currents ($|eV/kT_e| > 5$) with the tangent to the I-V curve at the origin of coordinates. In the idealized situation illustrated in Fig. 1 this procedure leads to values of i_1 and i_2 that are approximately 7% larger than those that would result using the procedure suggested in Ref. 2.
8. K. M. Burrows, Australian J. Phys. 15, 162 (1962).

9. E. W. Peterson and L. Talbot, AIAA 8, 2215 (1970).
10. E. W. McDaniel, Collision Pehnomena in Ionized Gases (John Wiley and Sons, New York, N.Y., 1964).
11. Frankenthal, American Science and Engineering Final Scientific Report ASE-1761/AFCRL 67-0607 (1967) (unpublished).
12. U. S. Standard Atmosphere Supplements, 1966.

FIGURE CAPTIONS

- Fig. 1. A schematic presentation of the experimental arrangement in the technique of the floating symmetric double-probe with its corresponding dimensionless current-voltage characteristic.
- Fig. 2. Correction term applicable to the original analysis scheme of Ref. 2 for the determination of electron temperature from the current-voltage characteristic of a symmetric double-probe system.
- Fig. 3. Schematic illustration of the electronics system employed in the ionospheric application of the floating double-probe technique.
- Fig. 4. Symmetric double-probe configuration on the Nike-Cajun (NASA 10.378) payload launched from White Sands, New Mexico.
- Fig. 5. Sample data from that collected by the symmetric double-probe in a lower-ionospheric application.
- Fig. 6. Current-voltage characteristic corresponding to the data shown in Fig. 5.

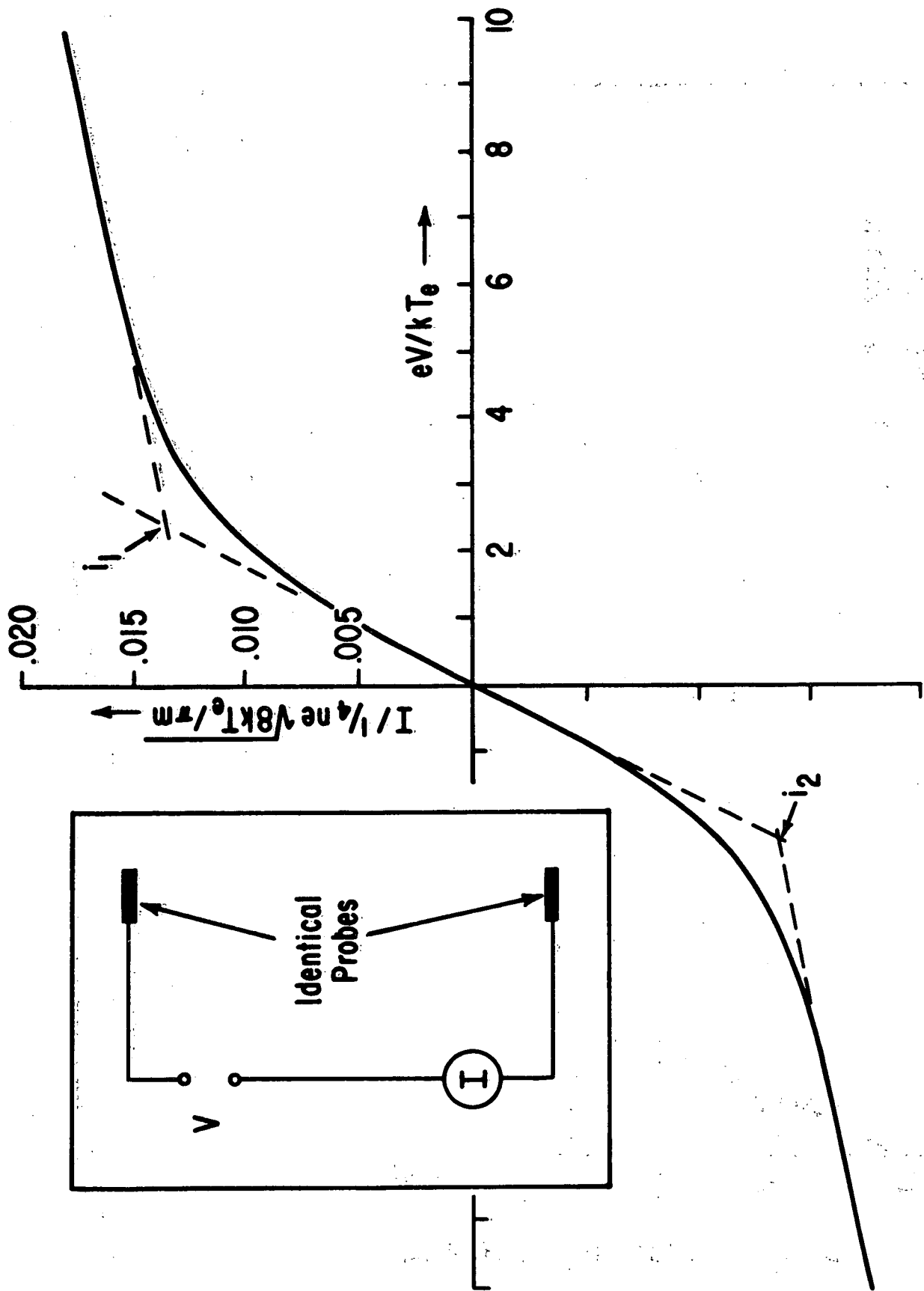


Fig. 1

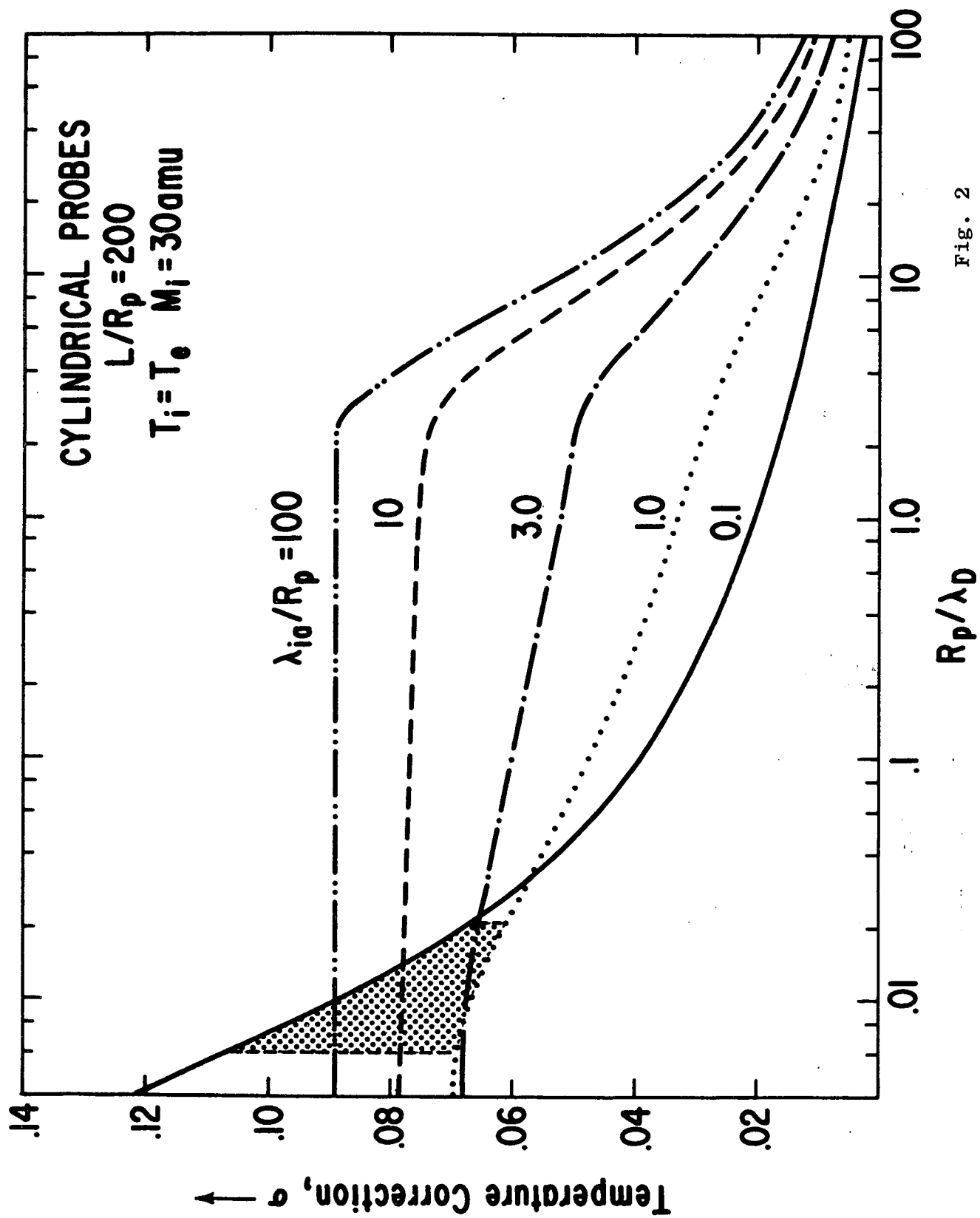


Fig. 2

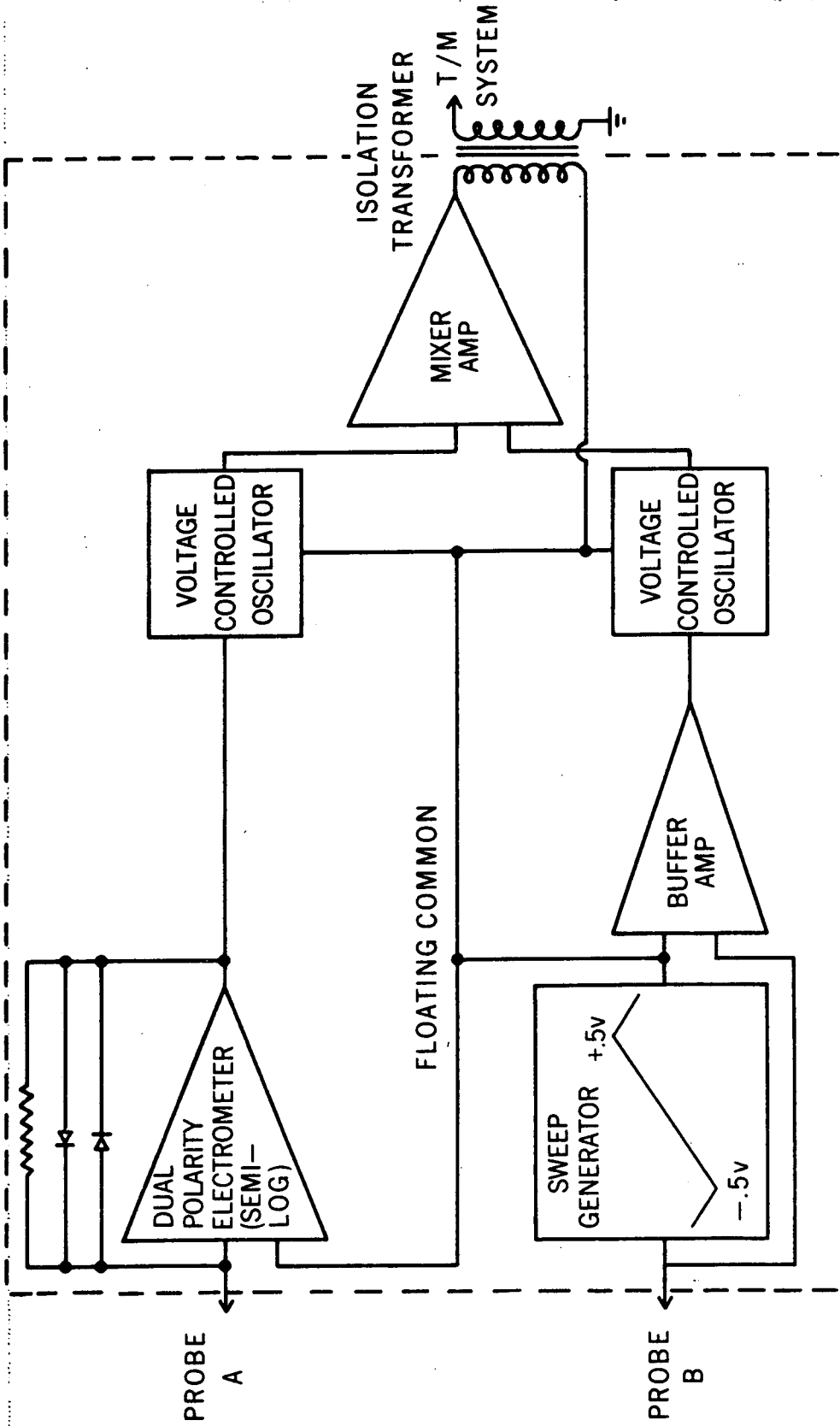


Fig. 3

FRONT - END VIEW

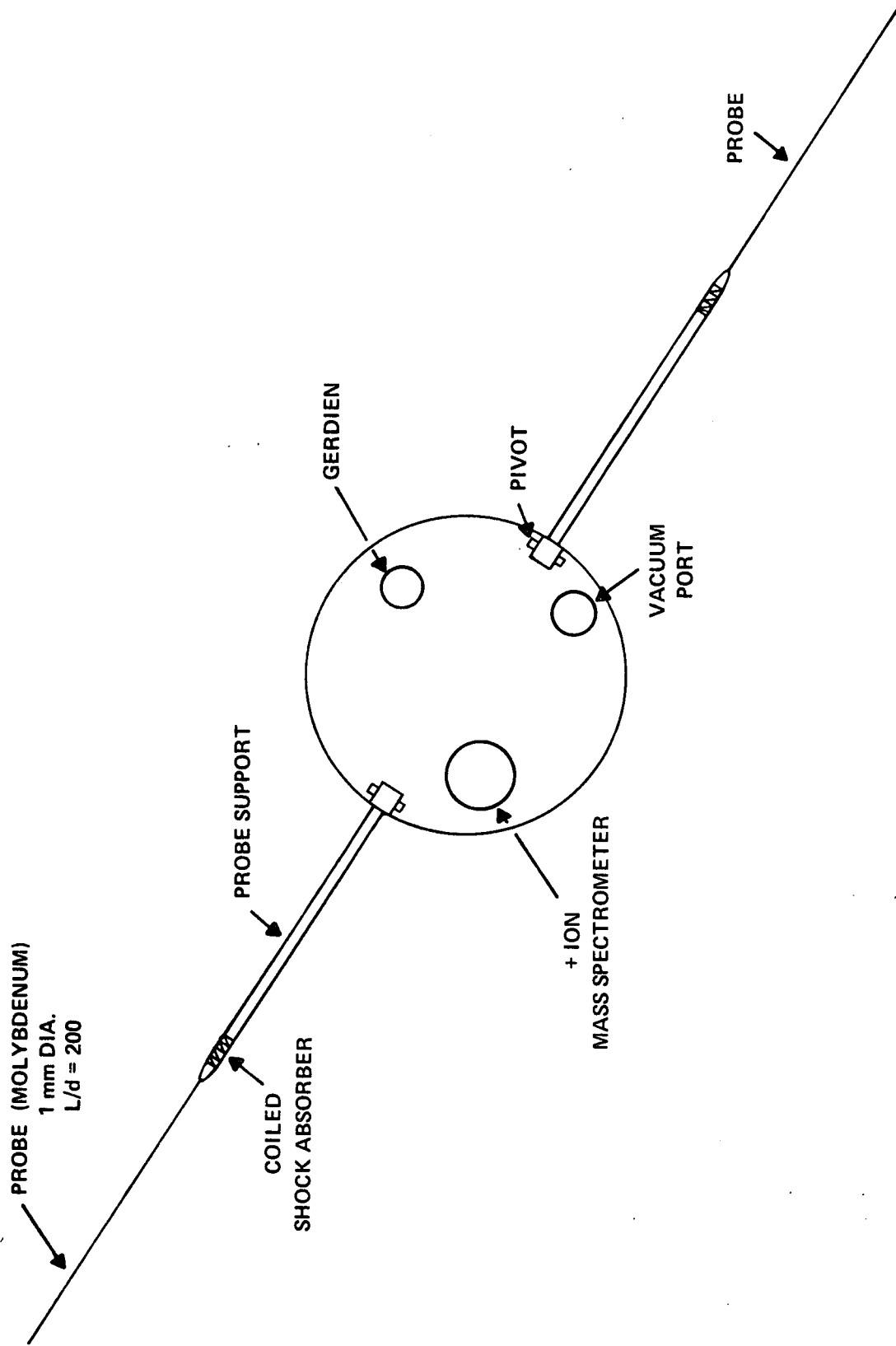


Fig. 4

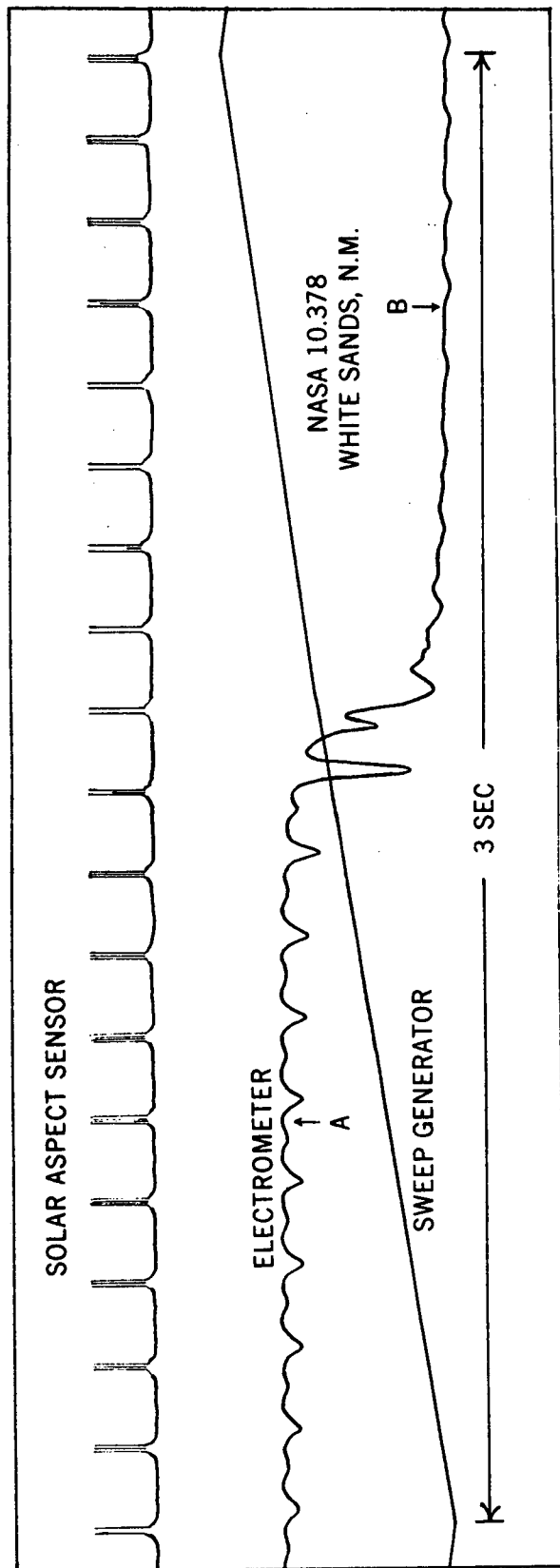


Fig. 5

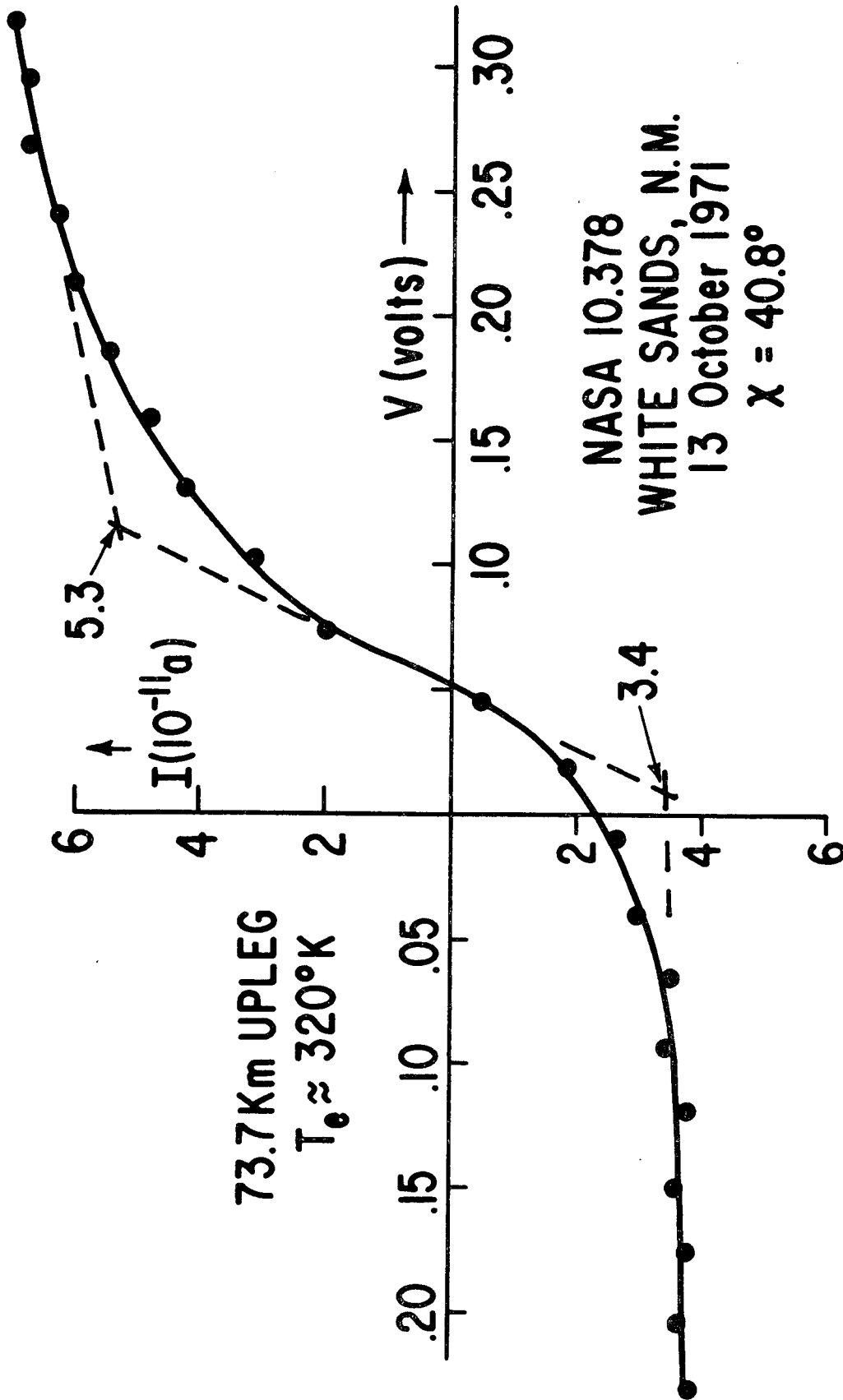


Fig. 6